scientific reports

Check for updates

OPEN

Antioxidant and anticancer properties of fucoidan isolated from *Saccharina Japonica* brown algae

Qiulin Yue[1,2]✉, Yongxuan Liu[1], Fujia Li[2], Tao Hong[4], Shousen Guo[1], Mengrui Cai[1], Lin Zhao[1], Le Su[1], Song Zhang[1], Chen Zhao[1] & Kunlun Li[3]✉

Fucoidan is a fucose-rich sulfated polysaccharide that has gained attention owing to its various biological activities. In this study, fucoidan was isolated from *Saccharina japonica* using an enzyme-assisted method, and its antioxidant and anti-hepatocarcinoma effects were evaluated. The fucoidan was a 112.8 kDa polysaccharide comprising seven monosaccharides: fucose, xylose, glucuronic acid, rhamnose, glucose, mannose, and galactose. The main chain residues were (1 → 3)-α-L-Fuc*p* and (1 → 4)-α-L-Fuc*p* units with sulfate groups at the C-2/C-4 positions of the (1 → 3)-α-L-Fuc*p* residues. *S. japonica* fucoidans showed excellent antioxidant potency with values of 1.02 mg TE/g and 5.39 mg TE/g for the ABTS and FRAP assays, respectively. Additionally, they exerted antitumor efficacy and low systemic toxicity in H22 tumor-bearing mice, with a tumor inhibition rate of 42.93%. Furthermore, it significantly inhibited tumor angiogenesis and reduced pro-inflammatory cytokines levels (IL-1β, IL-6, and TNF-α). Our results suggest that fucoidan isolated from *S. japonica* possesses potent antioxidant and anticancer properties and may be used as a potential agent for hepatocellular carcinoma treatment.

Keywords *Saccharina Japonica*, Fucoidan, Antioxidant, Anticancer, Angiogenesis

Hepatocellular carcinoma (HCC) is among the most prevalent cancers globally, characterized by high mortality and morbidity, resulting in approximately 830,000 deaths each year[1,2]. In 2020, nearly 1 million individuals worldwide were diagnosed with liver cancer, with HCC being the most common type[3]. While chemotherapy remains an effective treatment for HCC, its severe toxicity and the rapid development of drug resistance often led to an adverse prognosis or reduced sensitivity to chemotherapy[4]. Therefore, developing a potent HCC suppressor without toxic side effects is a promising therapeutic strategy for HCC treatment. Seaweed is an important marine biological resource that has been identified as one of the 50 foods that could help transform the global food system[5]. Particularly, brown algae contain various bioactive compounds, including sulfated polysaccharides, proteins, polyphenols, vitamins, dietary fibers, and fatty acids, which contribute to their nutritional and pharmaceutical properties[6]. Several studies have incorporated brown algae or their extracts into food matrices to develop highly nutritious food products[7,8]. Fucoidans are the most popular natural compounds found in brown algae because of their low toxicity and diverse medicinal properties[9]. Recently, fucoidan has been developed in various systems to improve and optimize the use of fucoidan in drug delivery, particularly in the field of cancer[10,11].

Fucoidans are sulfated heteropolysaccharides that primarily contain L-fucose and sulfate groups, uronic acid, and other monosaccharides, such as glucose, xylose, galactose, and mannose[12]. Generally, fucoidans comprise a backbone of α-(1–3)-linked fucose units or alternating α-(1–3) and α-(1–4) units of fucose residues[13]. The sulfate group is mostly substituted at the O-2, O-3, and O-4 positions[14]. The biological activity of fucoidan is dependent on its chemical composition, including molecular weight, monosaccharide composition, degree of sulfation, and position of the sulfate group[15]. In addition, the composition of fucoidans depends on the source of the algae, geographic location, and extraction and purification methods[16–18]. Traditional fucoidan extraction techniques,

[1]State Key Laboratory of Biobased Material and Green Papermaking, Shandong Provincial Key Laboratory of Microbial Engineering, Qilu University of Technology (Shandong Academy of Sciences), Jinan 250353, China. [2]Shandong Xiaoying Biotechnology Co., Ltd., Jinan 250003, China. [3]Jinan Hangchen Biotechnology Co., Ltd., Jinan 250000, China. [4]College of Ocean Food and Biological Engineering, Jimei University, Xiamen 361021, China. ✉email: yueqiulin88@163.com; Li_kunlun@163.com

including acidic and hydrothermal methods, are time-consuming, highly toxic, and may affect the structure of fucoidan, thereby affecting its bioactivity[19]. Recently, enzyme-assisted fucoidan extraction techniques have been developed to overcome these shortcomings and to obtain intact structures[20,21].

Fucoidans have diverse biological activities, including anticoagulant, antioxidant, and antitumor activities, depending on their physicochemical properties[22–24]. The antioxidant capacity of fucoidan is influenced by its molecular weight and degree of sulfation. Higher molecular weight fucoidans tend to exhibit stronger antioxidant activities, as they possess more complex structures that can interact effectively with free radicals[25]. Moreover, the degree of sulfation is critical. Fucoidans with higher sulfate content have been shown to have enhanced radical scavenging abilities, which is essential for their antioxidant function[26]. In various studies, fucoidan has been tested in different biological models to evaluate its protective effects against oxidative damage. For example, fucoidan isolated from *Sargassum fusiforme* demonstrated significant protective effects against ethanol-induced oxidative damage in liver cells, highlighting its potential as a functional food ingredient for liver health[27]. Additionally, the antioxidant activity of fucoidan has been associated with its anticancer properties, as oxidative stress is a known factor in cancer progression[26,28].

Numerous studies have demonstrated that fucoidans have effective inhibitory effects on the proliferation and migration of various tumor cell lines, including breast, colon, and lung cancers[29]. The relationship between the structure of fucoidan and its anti-cancer properties is complex and multifaceted, influenced by several structural characteristics such as molecular weight, degree of sulfation, and monosaccharide composition. Studies indicate that a decrease in molecular weight enhances the bioavailability of fucoidan and its capacity to interact with cancer cells, resulting in more pronounced anti-tumor activities[30,31]. Higher levels of sulfation are often correlated with increased anticancer activity, as sulfate groups enhance the solubility and bioactivity of fucoidan and facilitate its interaction with cellular receptors and signaling pathways involved in cancer progression[31,32]. Additionally, variations in the ratios of monosaccharides can affect the binding affinity of fucoidan to cell surface receptors, thereby modulating its anti-cancer effects. For example, the presence of L-fucose is particularly important for the anti-cancer activity of fucoidan, as it is involved in the recognition and binding processes that trigger cellular responses in cancer cells[33,34]. Despite the growing interest in fucoidans, specific studies on the anti-hepatocarcinoma activity of promising compounds are limited because not all fucoidans possess the same biological responses. Therefore, the preparation of fucoidans with native structures and good biological activity is of great significance.

In this study, fucoidan from the brown alga *S. japonica* was isolated and characterized using an enzyme-assisted extraction method. Moreover, its antioxidant and anti-hepatocarcinoma activities of hepatoma 22 (H22) tumor-bearing mice were investigated. The purpose of this study was to better understand the structure–activity relationship of fucoidans and facilitate the future development of effective natural therapies for HCC.

Materials and methods

Chemicals and materials

Saccharina japonica (formerly *Laminaria japonica*) (Phaeophyceae) was purchased from Tulip Crown Foods Co., Ltd. (Fuzhou, China). *Saccharina japonica* were collected from the coastal waters of Xiapu, Fujian Province, China (latitude: 26.88°N, longitude: 120.00°E) during the mature growth stage in October 2022. The seaweed samples were identified based on morphological characteristics, including blade morphology, sporophyte structure, and reproductive features. Voucher specimens were deposited in the Herbarium of Algae at Qilu University of Technology under the accession number QLUT-SJ-2022-001. L-Fucose, D-galactose, D-glucose, D-glucuronic acid, D-mannose, L-rhamnose, D-xylose, and Trolox were obtained from Sigma-Aldrich (St. Louis, MO, USA). Trifluoroacetic acid (TFA), 1-phenyl-3-methyl-5-pyrazolone (PMP), and injectable cyclophosphamide (CTX) were purchased from Shanghai Aladdin Biochemical Technology Co., Ltd. (Shanghai, China). Folin–Ciocalteu phenol reagent, 2,2′-azino-bis (3-ethylbenzothiazoline-6-sulfonic acid) (ABTS), and tripyridyl triazine (TPTZ) were purchased from Shanghai Macklin Biochemical Technology Co., Ltd. (Shanghai, China). ELISA detection kits for IL-1β, IL-6, TNF-α, carcinoembryonic antigen (CEA), and vascular endothelial growth factor (VEGF) were purchased from Jiangsu Meibiao Biotechnology Co., Ltd. All the other chemicals were of analytical grade.

Extraction and purification

S. japonica fucoidans were isolated using enzyme-assisted extraction. Enzymatic extracts of *S. japonica* was prepared using a previously reported method[35]. *S. japonica* was washed, dried, and ground, and the brown algal powder was passed through a 40-mesh screen and collected. The powder was dissolved in distilled water in a ratio of 1:30 (w/v). Subsequently, the pH was adjusted to 4.8, and Celluclast and pectinase were added at dry weights of 2.5% and 0.26%, respectively. The reaction solution was stirred at 50 °C for 2 h, and the pH was adjusted to 8.0, followed by the addition of alkaline pectinase (0.3%). The sample was incubated at 60 °C for another 1.5 h. Next, the reaction products were centrifuged, and the supernatants of the *S. japonica* extracts were collected.

The extracts were mixed with 35% $CaCl_2$ as a percentage of algal dry weight to precipitate alginic acid. Subsequently, the solution was centrifuged, and the collected supernatant was mixed with ethanol to a final ethanol concentration of 70% and stored at 4 °C overnight. The precipitate was collected and re-dissolved with the addition of ethanol at a ratio of 30% and stored at 4 °C. After incubation for 4 h, the solution was centrifuged, and the level of ethanol was modified to 70% and stored at 4 °C overnight. Finally, the fucoidan precipitate was obtained via centrifugal separation and lyophilization.

Chemical composition analysis

The total sugar content was analyzed using the phenol–sulfuric acid method, with L-fucose as the standard[36], and the sulfate group content was measured using the barium chloride–gelatin turbidity method[37]. The total polyphenol content was determined using the Folin–Ciocalteu method with gallic acid as the standard[38].

Analysis of monosaccharide composition

The monosaccharide composition of fucoidan was determined using pre-column high-performance liquid chromatography (Shimadzu LC-20 A, Japan) according to the literature, with certain modifications[39]. The polysaccharide sample was hydrolyzed with 4 M TFA at 110 °C for 2 h. After cooling to room temperature, the pH of the solution was adjusted to neutral, and the hydrolysate was mixed with 1 mL of 0.3 M NaOH and 1 mL of 0.5 M PMP–methanol solution, followed by incubation at 70 °C for 70 min. After cooling to room temperature, the solution was neutralized using 1 mL of 0.3 M acetic acid. Then, 0.1 M phosphate buffered saline (PBS) was added to the samples to reach a volume of 10 mL, and the solutions were extracted with 2.0 mL chloroform three times. The aqueous layer was then filtered through a 0.45-μm pore membrane filter and analyzed with an Agilent HC-C18(2) column (i.d. 5 μm, 4.6 mm × 250 mm). The column was set at 40 °C with a flow rate of 1.0 mL/min. The mobile phase comprised two solvents: solvent A (15% of acetonitrile (v/v) with 85% of 50 mM PBS at pH 6.9) and solvent B (40% of acetonitrile (v/v) with 60% of 50 mM PBS at pH 6.9). The solvent gradient in volumetric ratios was set as follows: 0–9.0 min, 8% B; 9.0–25.0 min, 20% B; 25.0–45.0 min, 25% B; and 45.0–55.0 min, 0% B. The UV absorbance of the effluent was monitored at a wavelength of 250 nm. The standard monosaccharides used were L-fucose, D-galactose, D-glucose, D-glucuronic acid, D-mannose, L-rhamnose, and D-xylose. The quantitative composition of the monosaccharides was calculated via comparison with reference sugars.

Molecular weight determination

Molecular weight was determined using a high-performance liquid chromatography system (Agilent 1260 Infinity II, Santa Clara, CA, USA) with a PL aquagel-OH Mixed-H column (i.d. 8 μm, 7.5 mm × 300 mm). The mobile phase was a 0.1 M $NaNO_3$ solution with 0.01% NaN_3. The sample was filtered through a 0.22-μm filter membrane before the analysis. The detection was conducted at a flow rate of 1.0 mL/min with a refractive index detector (Agilent 1260 Infinity II, Santa Clara, CA, USA). Six dextran's with different molecular weights (200, 100, 20, 40, 10, and 4 kDa) were used as the standards.

Methylation and GC–MS analysis

Methylation analysis was performed as previously described, with certain modifications[40]. Briefly, a polysaccharide sample (2 mg) was dissolved in 0.5 mL of dimethyl sulfoxide (DMSO) and permethylated using a fine NaOH/DMSO suspension (0.6 mL) and methyl iodide (0.6 mL). The reaction mixture was extracted with chloroform, and methyl iodide and chloroform were removed via evaporation. The methylated polysaccharides were hydrolyzed with 2 M TFA at 110 °C for 6 h, reduced with $NaBH_4$, and acetylated with acetic anhydride. Subsequently, partially methylated alditol acetates were analyzed using GC–MS (Agilent 7890B-5977B, Santa Clara, CA, USA) with a J&W HP-5ms capillary column (0.25 mm × 30 m, 0.25 μm, Agilent Technologies, Santa Clara, CA, USA). The compounds corresponding to each peak were identified by interpreting their characteristic mass spectra and comparing them to references. Peak areas were used to calculate the molar ratio of each residue.

Spectroscopy analysis

The dried fucoidan sample was ground with potassium bromide (KBr), and the mixture was pressed into pellets for FT-IR measurements. The spectrum was recorded with a Thermo Scientific Nicolet 380 FTIR spectrometer (Thermo Fisher Scientific, Waltham, MA, USA) over a wavelength range of 400–4000 cm^{-1} with KBr as the baseline.

The one-dimensional NMR spectra (^1H NMR, ^{13}C NMR) and 2D-NMR (^1H-^1H COSY, HSQC, HMBC and NOESY) were recorded using a Varian INOVA 600 NMR spectrometer (Varian Medical Systems, Palo Alto, CA, USA).

In vitro antioxidant assays

ABTS radical cation scavenging assay

The ABTS assay was conducted according to the method described by Fiol et al.[41], with certain modifications. ABTS reagent was generated by mixing 2.5 mL of 7.4 mM ABTS solution with 44 μL of 2.6 mM potassium persulfate overnight at 25 °C in the dark. The ABTS radical cation solution was further diluted with methanol to obtain an absorbance of 0.7 ± 0.05 at 734 nm. To determine the scavenging activity, 100 μL of ABTS reagent was mixed with 100 μL of various concentration sample solutions. The absorbance was measured at 734 nm using an ELISA reader (Molecular Devices, San Jose, CA 95134) after an exact reaction time of 6 min, and a calibration curve for Trolox was obtained. Results were expressed as milligram of Trolox equivalents per gram of extract (mg TE/g).

Ferric reducing antioxidant potential (FRAP) assay

The ferric reducing power of fucoidan was determined using a modified method of the FRAP assay by monitoring the reduction of a colorless Fe^{3+}-TPTZ solution to a blue-colored Fe^{2+}-TPTZ solution[42]. The working FRAP reagent was prepared by mixing 10 volumes of 300 mM acetate buffer (pH 3.6) with 1 volume of 10 mM TPTZ in 40 mM HCl and 1 volume of 20 mM ferric chloride. Subsequently, 100 μL of sample solutions and 300 μL of deionized water were added to 3 mL of freshly prepared FRAP reagent. The reaction mixture was incubated for 10 min at 37 °C, and the absorbance of the samples was measured at 593 nm on a UV-Vis spectrophotometer

(Hitachi U 2910, Kyoto, Japan). Results were expressed as milligram of Trolox equivalents per gram of extract (mg TE/g).

In vivo antitumor activity analysis

Cell culture

Mouse H22 cells were obtained from Procell Life Science and Technology Co., Ltd. (Wuhan, China). The cells were cultured in RPMI 1640 medium containing 10% FBS, 100 U/mL penicillin, and 0.1 mg/mL streptomycin and were maintained at 37 °C in a humidified incubator with a 5% CO_2 concentration.

Animals and antitumor efficacy in vivo

Four-week-old male ICR mice were obtained from Beijing Vital River Laboratory Animal Technology Co., Ltd. (Beijing, China). The mice were maintained at standard humidity and room temperature with a 12 h dark/light cycle and acclimatized for one week. All experimental procedures were performed under ARRIVE guidelines for the Care and Use of Laboratory Animals and approved by the Animal Ethics Committee of Qilu University of Technology (Shandong Academy of Sciences) (No. SWS20230303). All experiments were performed in accordance with relevant guidelines and regulations. H22 cells in the logarithmic growth phase were collected, and the cell density was adjusted to 2×10^6 cells/mL with the medium. The cell suspension (0.2 mL) was intraperitoneally injected into the right flank of the mice to establish a tumor model. When the tumors reached approximately 100 mm^3, the mice were randomly divided into four groups ($n = 6$): normal control (NC), model (M), cyclophosphamide (CTX), and fucoidan (FUC) groups. Mice in the CTX group were treated intraperitoneally with CTX (25 mg/kg body weight/day), serving as the positive control. In contrast, mice in the FUC group were orally administered fucoidan (100 mg/kg body weight/day). Sterile normal saline was orally administered to mice in the NC and M groups. Different formulations were administered daily for 15 d, and the body weights of the mice in each group were monitored. At the end of the experiment, blood was collected from the orbital vein under anesthesia with tribromoethanol (0.2 mL/10 g), and then the mice were sacrificed by cervical dislocation. Tumor tissues and organs, including the heart, liver, spleen, lungs, kidneys, and thymus, were immediately removed, washed with precooled sterile normal saline, dried, and weighed. The tumor tissues were stored at − 80 °C for histological analysis, and the organ index was calculated according to the following equation:

$$\text{Organ index} = \text{organ weight (mg)}/\text{body weight (g)}$$

Histopathological analysis

Tumor tissue samples were fixed in optimal cutting temperature embedding medium. Briefly, 8-μm thick sections were prepared and then stained with hematoxylin and eosin (H&E). Histopathological changes in liver tissues were observed under a light microscope (Olympus BX53, Japan).

Real-time PCR

Total RNA was extracted from the tumor tissue samples using the TRIzol reagent (BioFlux, Hangzhou, China). Reverse transcription was performed using a reverse transcription kit (ABclonal, Wuhan, China), and quantitative RT-PCR was performed using SYBR Green Fast Q-PCR (ABclonal, Wuhan, China) according to the manufacturer's instructions. The primer sequences are listed in Table 1. The β-actin housekeeping gene was used as a reference, and the relative quantification of mRNA level was determined using the $2^{-\Delta\Delta Ct}$ method.

ELISA assay

Serum CEA and VEGF levels were determined using ELISA kits according to the manufacturer's instructions. Inflammatory cytokine levels in serum, including IL-1β, IL-6, and TNF-α, were evaluated and calculated using mouse ELISA kits (Meibiao Biotechnology Co., Ltd., Jiangsu, China) according to the manufacturer's instructions.

Statistical analysis

Data are expressed as mean ± SD ($n = 6$). Statistical comparisons between groups were performed using one-way ANOVA and Duncan's multiple comparison test with GraphPad Prism software (Version 5.0). Statistical significance was set at $p < 0.05$.

Gene	Forward primer (5′–3′)	Reverse primer (5′–3′)
VEGF	F: TAGACGTTCCCTGCCAGCAA	R: AGCATCCGAGGAAAACATAAAATCTT
PI3K	F: GCGTGACATGTAGGCTCTCG	R: GGGCAGTGCTGGTGGAT
AKT1	F: CCGCCTGATCAAGTTCTCCT	R: TTCAGATGATCCATGCGGGG
mTOR	F: TACATTGGCTGGTGTCCCTTC	R: CTTAGCCATGTTGGCCCATCC
β-actin	F: CGCAGCCACTGTCGAGTC	R: GTCATCCATGGCGAACTGGT

Table 1. Primer sequences designed for this study.

Results

Chemical compositions and free radical-scavenging activities of fucoidan

The extraction yield based on dry seaweed weight was 2.44% ± 0.06%. The chemical compositions and free radical-scavenging activities of the purified polysaccharides were determined. As shown in Table 2, the contents of polysaccharides, sulfates, and polyphenols in fucoidan were 77.56% ± 1.45%, 17.85% ± 1.03%, and 0.15% ± 0.03%, respectively. The antioxidant activity of fucoidan was analyzed using ABTS radical cation scavenging and FRAP assays. The antioxidant capacities of the compounds were calculated as millimoles of Trolox equivalents per gram of extract. The results revealed that fucoidan showed excellent antioxidant activity with values of 1.02 and 5.39 mg TE/g for ABTS and FRAP assays, respectively.

Structural characterization of fucoidan

To further characterize the structure of fucoidan, a monosaccharide composition analysis was conducted. As shown in Fig. 1A, *S. japonica* fucoidans comprised seven monosaccharides: fucose, xylose, glucuronic acid, rhamnose, glucose, mannose, and galactose, with fucose (26.92%) and galactose (19.87%) as the primary monosaccharide components. Figure 1B shows that the average molecular weight of fucoidan was 1.128×10^5 g/mol. The proportion of principal components in the fucoidan was 76.8% according to the HPGPC results. Furthermore, methylation and GC–MS analyses have been conducted to determine the sugar links[43,44]. As shown in Table 3; Fig. 1D, the primary partially methylated alditol acetates were ascribed to 2,4-di-O-methylfucitol and 2,3-di-O-methylfucitol, which indicated the fucoidan was composed of (1 → 3)- and (1 → 4)-linked fucose residues as the main chain[45–47]. In addition, the galactose residues were present in the form of →4)- Gal*p*-(1→ and →6)- Gal*p*-(1→[44].

The FTIR analysis of fucoidan isolated from *S. japonica* is shown in Fig. 1C. The bands at 3389 and 2946 cm^{-1} were attributed to the stretching vibrations of O–H and C–H, respectively. The absorptions at 1626 and 1421 cm^{-1} were ascribed to the asymmetric and symmetric stretching vibrations of C=O, respectively[48]. The absorptions at 1218 and 823 cm^{-1} were assigned to the C–O–S bending vibration of the sulfate ester in the axial position and the S=O stretching vibration of the sulfate group, respectively[49,50]. The infrared peak at approximately 1025 cm^{-1} represented the stretching vibration of a glycosidic bridge (C–O–C)[51]. The ^{1}H NMR and ^{13}C NMR spectrum analysis results for fucoidan are shown in Fig. 1E and F. Owing to its structural complexity, fucoidan has a complex ^{1}H NMR spectrum, which is difficult to completely interpret. The signals at 1.25 and 1.33 ppm were assigned to the C6 methyl protons of L-fucopyranose. It included the characteristic resonances of the ring protons (H2-H5) between 3.6 and 4.8 ppm. The signals between 4.38 and 5.31 ppm corresponded to the anomeric protons of various sugar residues. However, there is significant overlap in the anomeric regions. Compared with the HSQC spectrum (Fig. S2), six anomeric proton signals were observed at 5.31, 5.29, 5.22, 4.83, 4.63 and 4.47 ppm, named A-F. The peak at 5.31 ppm in the spectrum of fucoidan was assigned to →3)- α-L-Fuc*p*2,4 diSO_4^{2-}-(1→3)-[52]. The signals at 5.29 was from the non-sulfated fucose residues→4)-α-L-Fuc*p*-(1→[40]. The anomeric proton signals at 4.83, 4.63, and 4.47 ppm were assigned to rhamnose, mannose, and galactose residues, respectively[48,53,54]. Accordingly, the chemical shifts of C1 of residue A-F can be obtained in the HSQC spectrum as 98.51, 99.45, 100.15, 99.45, 101.09 and 102.97 ppm. Moreover, the signal at 175.30 ppm was assigned as carbonyl carbon (C = O), which was consistent with FT-IR results. The ^{1}H and ^{13}C signals in residues A-F were listed in Table 4 on the basis of COSY, HSQC, NOESY and HMBC analysis (Figs. S1–S4 in Supplementary information), which was confirmed by comparing with data reported previously[48,52–54].

In vivo antitumor efficacy of fucoidan

The anti-tumor effects of the fucoidan were evaluated in H22 tumor-bearing mice. As shown in Fig. 2A,B, reductions in tumor volumes were observed in the FUC group compared to that for the M group. The inhibition rate in the FUC group was 42.93%, and significant antitumor effects were detected in the FUC and CTX groups (Table 5). Figure 2C shows the body weight variation in each group during administration. Compared with the NC group, the body weights of the M and CTX groups decreased owing to the influence of the tumor and toxicity of CTX. In contrast, mice treated with fucoidan displayed negligible weight loss compared with the NC group.

To further determine the anti-tumor efficacy in vivo, H22 solid tumors were sliced and stained with H&E. As shown in Fig. 2D, the tumor cells in the M group exhibited morphological characteristics with an oval or round shape, high density, and few infiltrations, indicating that the tumor cells were in good growth status. In contrast, the tumor cells became scattered and showed obvious chromatin condensation and few infiltrations in both the CTX and FUC groups. These results further confirmed that fucoidan effectively suppressed tumor cell growth. In addition, the organ index was analyzed to evaluate the potential toxicity of fucoidan. The histological photos and organ indices of major organs, including the heart, liver, spleen, lung, kidney, and thymus, in each group are presented in Fig. 2E,F. The thymus and spleen indices, which reflect the immune toxicity of antitumor agents, were determined. The spleen index significantly increased in the M group owing to tumor growth, whereas a normal spleen index value was observed in the FUC group. Fucoidan did not cause noticeable damage to normal organs compared with the NC group, indicating good biocompatibility and low toxicity.

Chemical composition (%)			TEAC	FRAP
Polysaccharide (%)	Sulfate (%)	Polyphenol (%)	(mg TE/g)	(mg TE/g)
77.56% ± 1.45	17.85% ± 1.03	0.15% ± 0.03	1.02 ± 0. 02	5.39 ± 0.14

Table 2. Chemical composition and antioxidant activities of fucoidan. Data are expressed as the mean ± SD.

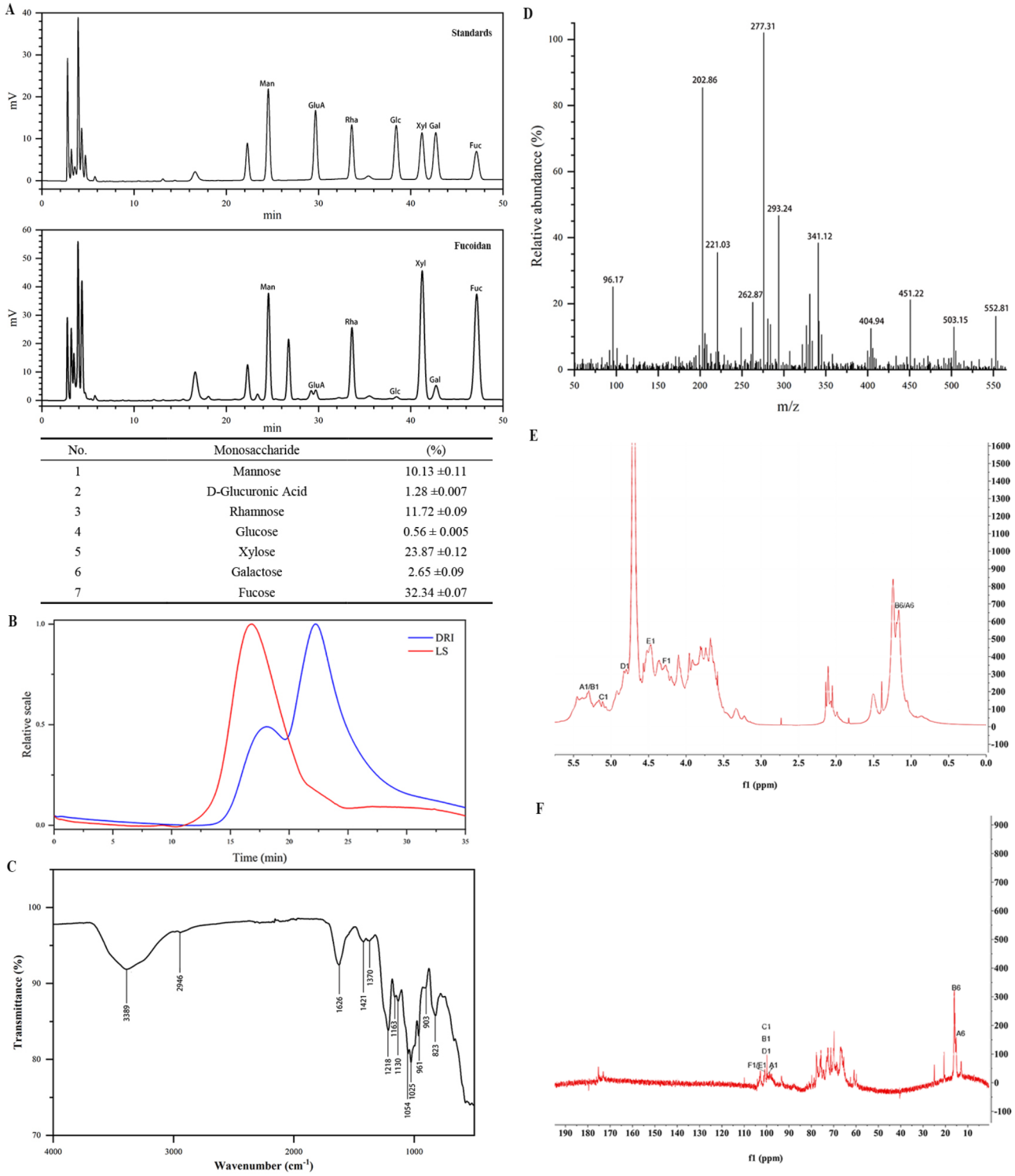

No.	Monosaccharide	(%)
1	Mannose	10.13 ±0.11
2	D-Glucuronic Acid	1.28 ±0.007
3	Rhamnose	11.72 ±0.09
4	Glucose	0.56 ± 0.005
5	Xylose	23.87 ±0.12
6	Galactose	2.65 ±0.09
7	Fucose	32.34 ±0.07

Fig. 1. Structural characterization results of fucoidan. (**A**) HPLC, (**B**) HPGPC, (**C**) FTIR, (**D**) GC-MS, (**E**) ^{1}H NMR and (**F**) ^{13}C NMR analysis. *Note*: DRI, Differential Refractive Index Detector; LS, Light Scattering Detector.

Effect of fucoidan on the serum levels of CEA and VEGF

CEA is a key marker of tumor burden and prognosis. As shown in Fig. 3A, the serum CEA level was significantly elevated in the M group compared to that in the NC group. The treatment of H22 tumor-bearing mice with fucoidan induced a significant reduction in CEA levels. The VEGF plays a crucial role in angiogenesis. Fucoidan treatment reduced the levels of VEGF in the serum, suggesting a tumor angiogenesis-inhibitory effect of the compound (Fig. 3B).

Peak	PMAA	Deduced linkage	Composition (mol%)
1	2-Me-Fuc	→3,4)-Fuc*p*-(1→	1.52
2	2,4-Me_2-Fuc	→3)-Fuc*p*-(1→	28.81
3	2,3-Me_2-Fuc	→4)-Fuc*p*-(1→	14.29
4	2,4-Me_2-Rha	→3)- Rha*p*-(1→	2.07
5	2,4-Me-Man	→3,6)-Man*p*-(1→	1.12
6	2,4,6-Me_3-Man	→3)-Man*p*-(1→	0.83
7	2,3,4-Me_3-Gal	→6)-Gal*p*-(1→	0.95
8	2,3-Me_2- Gal	→4)- Gal*p*-(1→	10.62
9	3-Me-Xyl	→2,4)-Xyl*p*-(1→	2.38

Table 3. Results of the methylation analysis of fucoidan.

Residue	H1/C1	H2/C2	H3/C3	H4/C4	H5/C5	H6/C6
A →3)- α-L-Fucp2S4S-(1→	5.31/98.51	4.56/77.65	5.08/71.19	4.48/73.19	4.08/71.25	1.18/15.52
B →4)-α-L-Fucp-(1→	5.29/99.55	3.97/72.26	4.73/77.18	4.01/69.91	4.24/66.86	1.14/19.16
C →2)-α-D-Manp-(1→	5.22/100.15	3.75/71.08	4.64/77.05	3.65/72.29	4.30/73.66	3.58/62.41
D →3)-β-L-Rhap-(1→	4.83/99.45	4.52/80.93	3.92/72.26	4.48/75.07	3.82/76.01	4.32/71.55
E →6)-β-D-Manp-(1→	4.63/101.09	3.74/82.57	4.37/73.19	3.89/76.01	4.12/75.77	3.67/71.32
F →6)-β-D-Galp-(1→	4.47/102.97	3.61/74.6	4.10/70.62	3.67/76.01	3.96/69.91	3.55/62.18

Table 4. Chemical shift assignments of fucoidan.

Effects of fucoidan on the gene expression of the PI3K/AKT/mTOR pathway

Next, we evaluated the effect of fucoidan on key pro-angiogenic pathways and detected the expression of VEGF and its downstream signaling molecules. As shown in Fig. 4, the results of our expression profiling analysis revealed concomitant significant downregulation of VEGF (0.66-fold), PI3K (0.71-fold), AKT1 (0.57-fold), and mTOR (0.58-fold) in the FUC group compared to that in the model tumor tissues. These results indicated that fucoidan exerts anti-tumor effects by deregulating PI3K/AKT/mTOR signaling during transcription.

Effect of fucoidan on the expression of inflammatory cytokines

Cytokines are critical components of tumor generation and development. As shown in Fig. 5, the expressions of IL-1β, IL-6, and TNF-α were increased in the M group compared to the NC group. However, treating H22 tumor-bearing mice with fucoidan significantly reduced the serum levels of these three cytokines. These results indicate that fucoidan inhibits tumor growth by regulating the expression of inflammatory cytokines in the serum.

Discussion

Recently, several studies have shown that fucoidans exhibit various biological activities with minimal toxicity, rendering them optimal candidates for cancer treatment[5,28,29]. The structure of fucoidan highly depends on the algal species and the extraction and purification methods. Two types of fucoidan backbones can be distinguished, including the (1 → 3)-linked-L-fucopyranose residues and alternating (1 → 3)-linked L-fucopyranose and (1 → 4)-linked L-fucopyranose residues[29]. Monosaccharide composition, sulfate content, and molecular weight are key factors associated with anticancer effects[55–57]. In recent decades, fucoidans have been extracted using water and acids. However, water extraction requires a long time, and acid treatment can affect the structure of fucoidans. Recently, several studies have reported enzyme-assisted mild extraction methods that can significantly reduce extraction time with a higher extraction yield[58,59].

In this study, we obtained *S. japonica* fucoidans using enzyme-assisted extraction, followed by calcium chloride and gradient alcohol precipitation. The yield of fucoidan obtained through water extraction was 1.24 ± 0.05 (data not shown). It is evident that enzyme-assisted extraction outperforms hot-water extraction in terms of yield. The results demonstrate that the incorporation of Celluclast and pectinase significantly enhanced the degradation of highly crystalline cellulose and facilitated the breakdown of the crosslinked networks within the cell wall, thereby effectively promoting the dissociation and release of fucoidan. Free radical scavenging activity was evaluated using ABTS and FRAP assays. Table 2 showed that the ABTS and FRAP radical scavenging activity of the fucoidan were 1.02 and 5.39 mg TE/g, respectively. It is reported that several fucoidans in brown algae (*Sargassum filipendula*, *Cladosiphon okamuranus*, *Sargassum horneri*, *Kjellmaniella crassifolia*, *Nemacystus decipiens*, and *Fucus vesiculosus*) have high antioxidant capacity, and their antioxidant capacity varies depending on the species (ranging from 1.15 to 4.50 mg Trolox/g fucoidan)[60]. The free radical scavenging activity of fucoidan is inconsistent, partly due to differences in the sulfate content of extracted fucoidan[61]. *S. japonica* fucoidans in the present study had high concentrations of total sugar and sulfate, but low concentrations of polyphenols. The results indicated that the extracted fucoidan with higher sulfate content had a significant antioxidant activity. Zeinab et al. reported that fucoidan demonstrated a high ABTS radical cation-scavenging capacity[62]. In contrast,

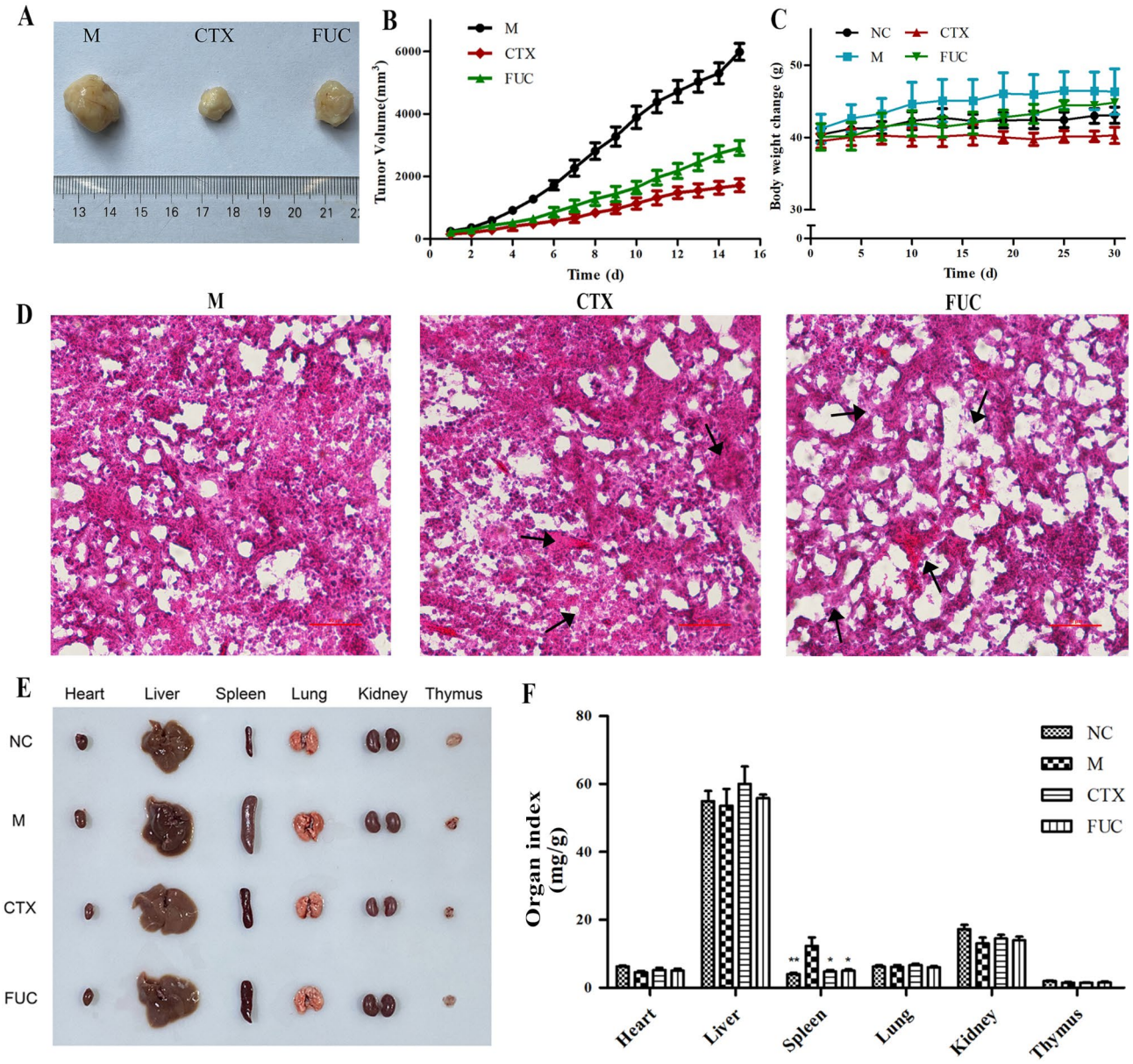

Fig. 2. Antitumor efficacy of fucoidan in tumor-bearing mice. (**A**) Photograph of tumors excised from different experimental groups. (**B**) Changes in tumor volume during intervention. (**C**) Body weight changes of mice in different experimental groups. (**D**) H&E-stained sections of tumor tissues (black arrows show the necrotic area). (**E**) Representative morphologic images of major organ tissues. (**F**) Organ index of mice in different experimental groups. $^{*}p < 0.05$, $^{**}p < 0.01$ represent a significant difference compared to the model group.

Group	Dosage (mg/kg)	Tumor weight (g)	Inhibition rate (%)
Model	–	1.99 ± 0.11	–
CTX	25	$0.84 \pm 0.07^{\#\#}$	57.58
Fucoidan	100	$1.04 \pm 0.07^{***}$	42.93

Table 5. Effect of fucoidan on the growth of H22 tumor tissues. Data are expressed as the mean ± SD. $^{***}p < 0.001$ represents a significant difference compared to the model group. $^{\#\#}p < 0.01$ represents a significant difference compared to the CTX group.

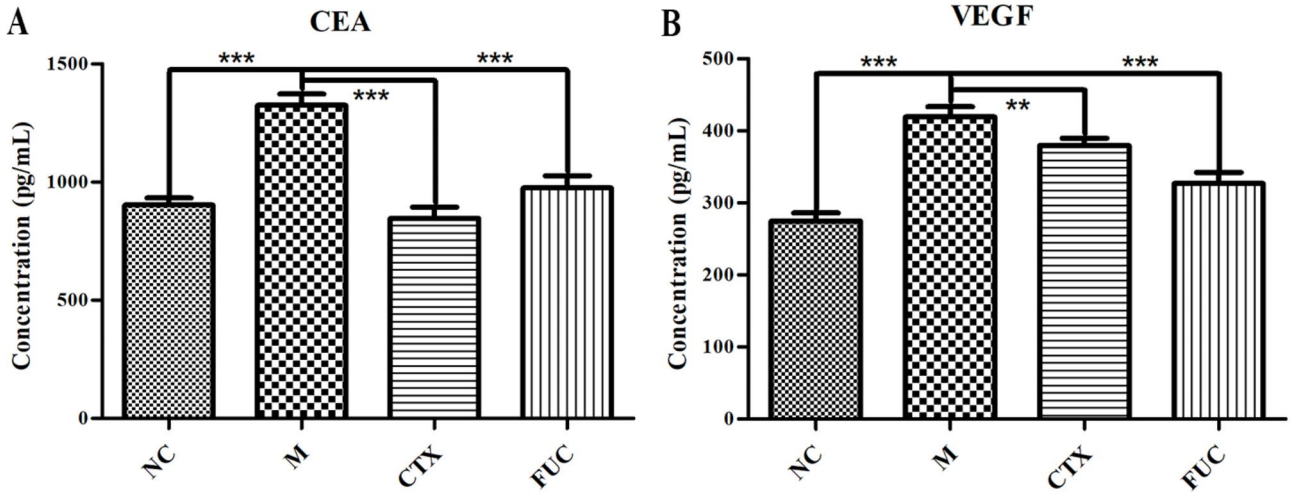

Fig. 3. Effects of fucoidan on CEA (**A**) and VEGF (**B**) levels in serum.

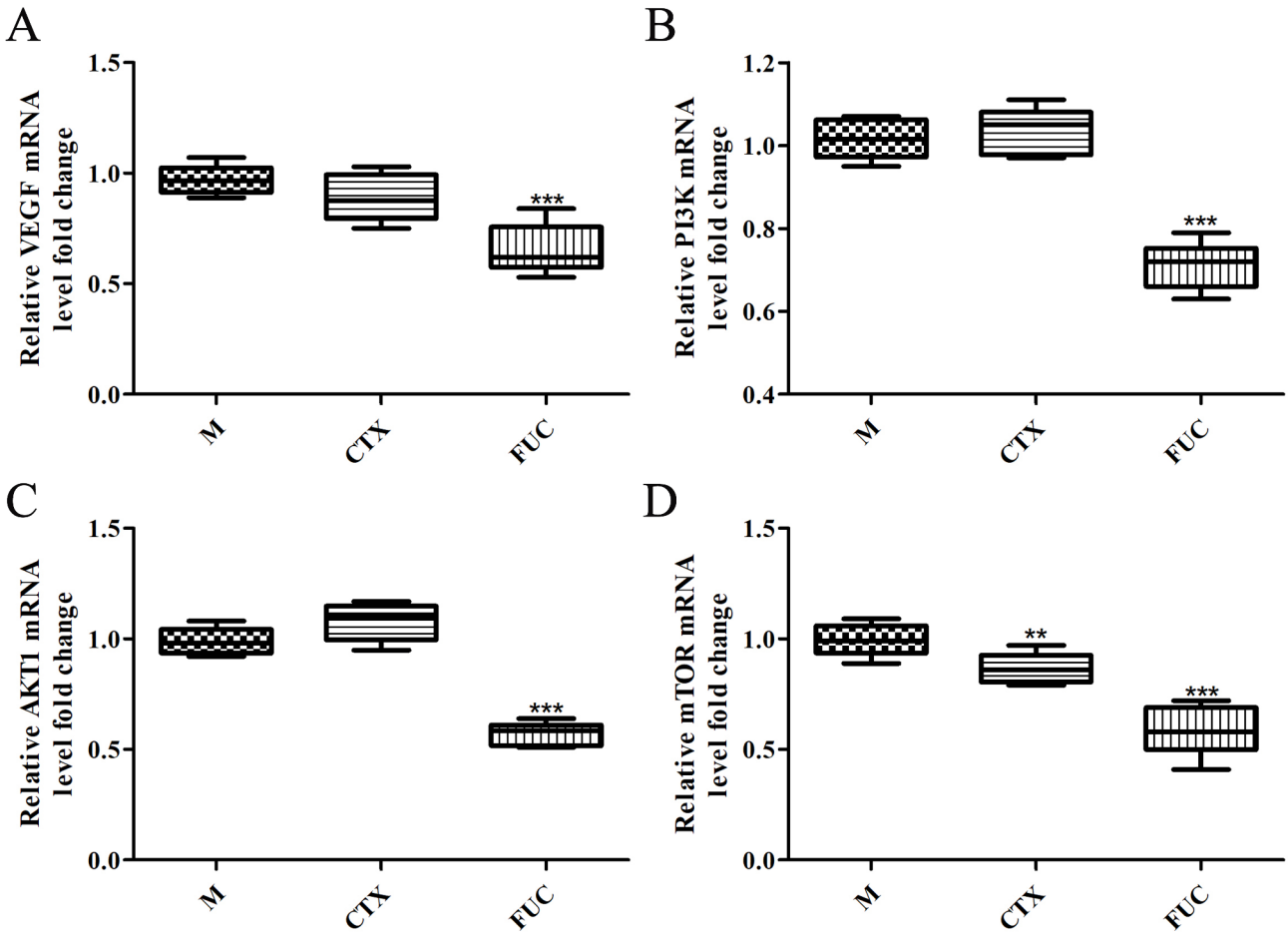

Fig. 4. Effects of fucoidan on the gene expressions in tumor tissues: (**A**) VEGF, (**B**) PI3K, (**C**) AKT1, and (**D**) mTOR.

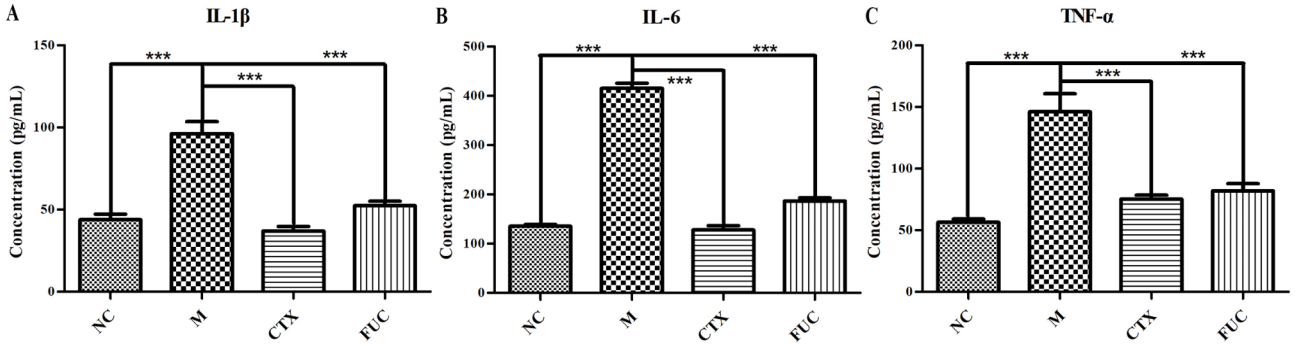

Fig. 5. Effects of fucoidan on the expression of inflammatory cytokines: (**A**) IL-1β, (**B**) IL-6, and (**C**) TNF-α.

our results revealed that *S. japonica* fucoidans exhibited better antioxidant activity in the FRAP assay than in the ABTS assay. Differences in reported data may be related to other structural factors such as the position of the sulfate group, monosaccharide composition, and backbone of the polysaccharide[63]. Therefore, the relationship between the microstructure and biological activity of the polysaccharides extracted by different methods needs further study.

The structures identified in this study were similar to those of other brown algal species, such as *Ishige okamurae*[40] and *Sargassum hemiphyllum* polysaccharides[64]. These polysaccharides contain (1→3)-Fucp and (1→4)-Fucp residues, with a sulfate group attached to the C-2 or C-4 position of fucose. However, there were significant differences in the monosaccharide content or proportions. *S. japonica* fucoidans comprised seven monosaccharides: fucose, xylose, glucuronic acid, rhamnose, glucose, mannose, and galactose, with fucose (26.92%) and galactose (19.87%) being the primary components. *S. japonica* fucoidans have been reported to contain the highest concentrations of fucose and galactose[58,65]. This finding aligns with the results of the present study. *Sargassum* fucoidans obtained using different extraction methods have different monosaccharide content, sulfate, and total sugar contents and antioxidant activities[66]. Enzyme-assisted extraction is a new strategy for mild fucoidan extraction that provides new opportunities to obtain natural fucoidan structures from brown algae in high yields[20]. The addition of Celluclast appears to significantly enhance the degradation of cellulose and hemicellulose that are highly cross-linked with fucoidan, which may explain the observed increase in galactose (19.87%) and mannose (8.51%). Fucoidans that are isolated using new enzymatic extraction techniques can be used to provide insights into different fucoidan structures and biological activities.

As a natural product, fucoidans are potential non-toxic agents for cancer treatment. Numerous studies have reported various antitumor activities of fucoidan in lung[67], colorectal[68], and breast cancers[69]. However, there has been limited research in anti-HCC therapy; therefore, further research is required. In this study, we evaluated the antitumor activity of fucoidan in an H22 tumor-bearing mouse model. These results confirmed that fucoidans significantly inhibit tumor tissue growth in H22 tumor-bearing mice without noticeable toxicity. Fucoidans from *Sargassum plagiophyllum* (Phaeophyceae) exhibit anticancer activity by inhibiting the activation of carcinogen metabolism in DEN-induced liver cancer[70]. A recent study also showed that the combination of algal fucoidans and anti-angiogenic drugs can significantly improve the therapeutic effect in liver cancer[71]. These studies indicate that fucoidan has great potential for clinical development as a drug or dietary supplement for liver cancer, owing to its relative safety and bioavailability.

CEA is a typical tumor marker in hepatocellular carcinoma, and serum CEA levels are reportedly elevated owing to cancer-induced damage[72]. In the present study, the serum level of CEA was significantly lower in fucoidan-treated mice than in the M group, demonstrating the antitumor effects of fucoidan. Tumor-induced angiogenesis also plays a critical role in solid tumor growth[73]. Therefore, the anti-angiogenic potential of antitumor agents has gained considerable attention in cancer treatment.

VEGF is a key angiogenic protein involved in tumor angiogenesis[74]. The published literature has revealed controversial results regarding the interaction between fucoidan and angiogenic pathways, particularly VEGF. Fucoidan inhibits HCC tumorigenesis without interfering with angiogenesis and VEGF expression both in vitro and in vivo[75]. In contrast, another study reported that fucoidan decreased the levels of VEGF, although the results were not significant compared to the untreated control[71]. In the current study, fucoidan treatment reduced the level of VEGF in the serum, suggesting its potential for tumor angiogenesis inhibition. These discrepancies in the bioactivities of the different fucoidans may be attributed to differences in their molecular weights and chemical structures.

The PI3K/AKT/mTOR signaling pathway plays an important role in cancer development[76,77]. Early studies confirmed that fucoidans regulate the proliferation of cancer cells through the PI3K/AKT pathway in lung[78] and colon cancers[31]. Similar regulation of the PI3K/AKT/mTOR signaling pathway was also observed in a DEN-induced HCC rat model following fucoidan treatment[71]. Our data provide additional support for the view that fucoidans may be involved in the regulation of the PI3K/AKT/mTOR signaling pathway to exert anti-cancer effects.

Immune-related cytokines play a vital role in regulating tumor generation and development[79]. Cytokines are crucial factors in tumor immunotherapy. TNF-α is a pro-inflammatory cytokine that can inhibit tumor cells, activate lymphocytes, and participate in the regulation of oncogenesis[80,81]. IL-1β and IL-6 are also important

cytokines that play a central role in liver carcinogenesis[82]. To investigate the immunomodulatory effect of fucoidans, the levels of IL-1β, IL-6, and TNF-α were measured using ELISA. Fucoidans significantly reduced pro-inflammatory cytokines IL-1β, IL-6, and TNF-α levels in H22 tumor-bearing mice. These results indicated that fucoidans inhibit tumor growth by regulating the expression of inflammatory cytokines.

In summary, we have established an efficient enzyme-assisted extraction method for fucoidans from *S. japonica* brown seaweeds, yielding high-purity, high-sulfate fucoidan. Our findings demonstrate that *S. japonica* fucoidans exhibit potent antioxidant and anticancer activities, with low immunotoxicity in the H22 tumor mouse model. Consequently, the enzyme-assisted extraction method is anticipated to effectively isolate authentic fucoidan with high bioactivity from brown algae, thereby enhancing our understanding of the bioactive roles of fucoidan structure. However, given the relatively complex structure of fucoidan, detailed studies are necessary to systematically investigate the relationship between its structure and efficacy. Additionally, studies that explore the combination of fucoidan with anticancer drugs may further elucidate its potential role in enhancing anticancer efficacy and reducing drug toxicity, thereby contributing to the knowledge regarding the clinical applicability of fucoidan.

Conclusion

Fucoidan was isolated from *S. japonica* and its structure was analyzed. The average molecular weight of the fucoidan was 1.128×10^5 g/mol. The polysaccharide comprised a main chain of (1 → 3)-α-L-Fuc*p* and (1 → 4)-α-L-Fuc*p* units, with sulfate groups at the C-2/C-4 positions of the (1 → 3)-α-L-Fuc*p* residues. *S. japonica* fucoidans exhibited potent antioxidant activity in vitro and antitumor activity in an H22 tumor-bearing mouse model with low immunotoxicity. This antitumor effect may be attributed to the inhibition of tumor angiogenesis and enhancement of the immune response. However, further studies are required to fully understand the anti-tumor mechanisms in vivo. Our results suggest the potential value of *S. japonica* fucoidans in the treatment of HCC.

Data availability

All data analysed during this study are included in this article and supplementary materials.

Received: 7 November 2024; Accepted: 12 March 2025
Published online: 15 March 2025

References

1. Zong, S. et al. Synergistic antitumor effect of polysaccharide from *Lachnum* Sp. in combination with cyclophosphamide in hepatocellular carcinoma. *Carbohydr. Polym.* **196**, 33–46. https://doi.org/10.1016/j.carbpol.2018.05.006 (2018).
2. Vairappan, B., Wright, G. & Ravikumar, T. S. Incidence, diagnosis, and management of hepatocellular carcinoma: Current perspectives and future direction. *J. Dig. Dis. Hepatol.* **8**, 188. https://doi.org/10.29011/2574-3511.100088 (2023).
3. Vogel, A. M. T., Sapisochin, G., Salem, R. & Saborowski, A. Hepatocellular carcinoma. *Lancet* **400**, 1345–1362. https://doi.org/10.1016/S0140-6736(22)01200-4 (2022).
4. Llovet, J. M. et al. SHARP investigators study group. Sorafenib in advanced hepatocellular carcinoma. *N. Engl. J. Med.* **359**, 378–390. https://doi.org/10.1056/NEJMoa0708857 (2008).
5. Tagliapietra, B. L. & Clerici, M. T. P. S. Brown algae and their multiple applications as functional ingredient in food production. *Food Res. Int.* **167**, 112655. https://doi.org/10.1016/j.foodres.2023.112655 (2023).
6. Park, E. et al. Seaweed metabolomics: A review on its nutrients, bioactive compounds and changes in climate change. *Food Res. Int.* **163**, 112221. https://doi.org/10.1016/j.foodres.2022.112221 (2023).
7. Arufe, S. et al. Effect of brown seaweed powder on physical and textural properties of wheat bread. *Eur. Food Res. Technol.* **244**, 1–10. https://doi.org/10.1007/s00217-017-2929-8 (2018).
8. Nuñez, M. & Picon, A. Seaweeds in yogurt and quark supplementation: Influence of five dehydrated edible seaweeds on sensory characteristics. *Int. J. Food Sci. Technol.* **52**, 431–438. https://doi.org/10.1111/ijfs.13298 (2017).
9. Sanjeewa, K. A., Lee, J. S., Kim, W. S. & Jeon, Y. J. The potential of brown-algae polysaccharides for the development of anticancer agents: An update on anticancer effects reported for fucoidan and laminaran. *Carbohydr. Polym.* **177**, 451–459. https://doi.org/10.1016/j.carbpol.2017.09.005 (2017).
10. Oliveira, C., Neves, N. M., Reis, R. L., Martins, A. & Silva, T. H. A review on fucoidan antitumor strategies: From a biological active agent to a structural component of fucoidan-based systems. *Carbohydr. Polym.* **239**, 116131. https://doi.org/10.1016/j.carbpol.2020.116131 (2020).
11. Oliveira, C. Fucoidan/chitosan nanoparticles functionalized with anti-ErbB-2 target breast cancer cells and impair tumor growth in vivo. *Int. J. Pharm.* **600**, 120548. https://doi.org/10.1016/j.ijpharm.2021.120548 (2021).
12. Li, J., He, Z. X., Liang, Y. M., Peng, T. & Hu, Z. Insights into algal polysaccharides: A review of their structure, depolymerases, and metabolic pathways. *J. Agric. Food Chem.* **70**, 1749–1765. https://doi.org/10.1021/acs.jafc.1c05365 (2022).
13. Barbosa, A. I., Coutinho, A. J., Costa Lima, S. A. C. & Reis, S. Marine polysaccharides in pharmaceutical applications: fucoidan and Chitosan as key players in the drug delivery match field. *Mar. Drugs* **17**. https://doi.org/10.3390/md17120654 (2019).
14. Zhao, X. et al. Antithrombotic activity of oral administered low molecular weight fucoidan from *Laminaria Japonica Thromb. Res.* **144**, 46–52. https://doi.org/10.1016/j.thromres.2016.03.008 (2016).
15. Ale, M. T., Mikkelsen, J. D. & Meyer, A. S. Important determinants for fucoidan bioactivity: A critical review of structure-function relations and extraction methods for fucose-containing sulfated polysaccharides from brown seaweeds. *Mar. Drugs* **9**, 2106–2130. https://doi.org/10.3390/md9102106 (2011).
16. Jin, W. H. et al. A study of neuroprotective and antioxidant activities of heteropolysaccharides from six *Sargassum* species. *Int. J. Biol. Macromol.* **67**, 336–342. https://doi.org/10.1016/j.ijbiomac.2014.03.031 (2014).
17. Mak, W., Hamid, N., Liu, T., Lu, J. & White, W. L. Fucoidan from new Zealand *Undaria pinnatifida*: Monthly variations and determination of antioxidant activities. *Carbohydr. Polym.* **95**, 606–614. https://doi.org/10.1016/j.carbpol.2013.02.047 (2013).
18. Rodriguez-Jasso, R. M., Mussatto, S. I., Pastrana, L., Aguilar, C. N. & Teixeira, J. A. Microwave-assisted extraction of sulfated polysaccharides (fucoidan) from brown seaweed. *Carbohydr. Polym.* **86**, 1137–1144. https://doi.org/10.1016/j.carbpol.2011.06.006 (2011).
19. Nguyen, T. T. et al. Enzyme-assisted fucoidan extraction from brown macroalgae *Fucus distichus* subsp. *Evanescens* and *Saccharina latissima*. *Mar. Drugs* **18**. https://doi.org/10.3390/md18060296 (2020).
20. Dörschmann, P. et al. Effects of a newly developed enzyme-assisted extraction method on the biological activities of fucoidans in ocular cells. *Mar. Drugs* **18**. https://doi.org/10.3390/md18060282 (2020).

21. Kirsten, N. et al. Impact of enzymatically extracted high molecular weight fucoidan on lipopolysaccharide-induced endothelial activation and leukocyte adhesion. *Mar. Drugs* **21**, 339. https://doi.org/10.3390/md21060339 (2023).
22. Atashrazm, F., Lowenthal, R. M., Woods, G. M., Holloway, A. F. & Dickinson, J. L. Fucoidan and cancer: A multifunctional molecule with anti-tumor potential. *Mar. Drugs* **13**, 2327–2346. https://doi.org/10.3390/md13042327 (2015).
23. Mansour, M. B. et al. Primary structure and anticoagulant activity of fucoidan from the sea cucumber *Holothuria polii*. *Int. J. Biol. Macromol.* **121**, 1145–1153. https://doi.org/10.1016/j.ijbiomac.2018.10.129 (2019).
24. Palanisamy, S., Vinosha, M., Marudhupandi, T., Rajasekar, P. & Prabhu, N. M. Isolation of fucoidan from *Sargassum polycystum* brown algae: Structural characterization, in vitro antioxidant and anticancer activity. *Int. J. Biol. Macromol.* **102**, 405–412. https://doi.org/10.1016/j.ijbiomac.2017.03.182 (2017).
25. Yu, J. et al. Fucoidan extracted from sporophyll of Undaria pinnatifida grown in Weihai, China—Chemical composition and comparison of antioxidant activity of different molecular weight fractions. *Front. Nutr.* **8**, 636930. https://doi.org/10.3389/fnut.2021.636930 (2021).
26. Pozharitskaya, O. N., Obluchinskaya, E. D. & Shikov, A. N. Mechanisms of bioactivities of fucoidan from the brown seaweed *Fucus vesiculosus* L. of the Barents sea. *Mar. Drugs*. **18**(5). https://doi.org/10.3390/md18050275 (2020).
27. Wang, L. et al. Protective effect of sargassum fusiforme fucoidan against ethanol-induced oxidative damage in in vitro and in vivo models. *Polym. (Basel)* **15**(8). https://doi.org/10.3390/polym15081912 (2023).
28. Shiau, J. P. et al. Brown algae-derived fucoidan exerts oxidative stress-dependent antiproliferation on oral cancer cells. *Antioxid. (Basel)* **11**(5). https://doi.org/10.3390/antiox11050841 (2022).
29. van Weelden, G. et al. Fucoidan structure and activity in relation to anti-cancer mechanisms. *Mar. Drugs* **17**. https://doi.org/10.3390/md17010032 (2019).
30. Fernando, I. P. S. et al. Fucoidan purified from sargassum polycystum induces apoptosis through mitochondria-mediated pathway in HL-60 and MCF-7 cells. *Mar. Drugs*. **18**(4). https://doi.org/10.3390/md18040196 (2020).
31. Han, Y. S., Lee, J. H. & Lee, S. H. Fucoidan inhibits the migration and proliferation of HT-29 human colon cancer cells via the phosphoinositide-3 Kinase/Akt/mechanistic target of Rapamycin pathways. *Mol. Med. Rep.* **12**, 3446–3452. https://doi.org/10.3892/mmr.2015.3804 (2015).
32. Blaszczak, W. et al. Fucoidan exerts anticancer effects against head and neck squamous cell carcinoma in vitro. *Molecules* **23**(12). https://doi.org/10.3390/molecules23123302 (2018).
33. Kim, I. H., Kwon, M. J. & Nam, T. J. Differences in cell death and cell cycle following fucoidan treatment in high-density HT-29 colon cancer cells. *Mol. Med. Rep.* **15**(6), 4116–4122. https://doi.org/10.3892/mmr.2017.6520 (2017).
34. Zhao, Y. et al. A transcriptome sequencing study on genome-wide gene expression differences of lung cancer cells modulated by fucoidan. *Front. Bioeng. Biotechnol.* **10**, 844924. https://doi.org/10.3389/fbioe.2022.844924 (2022).
35. Yue, Q. et al. Hypolipidemic effects of fermented seaweed extracts by *Saccharomyces cerevisiae* and *Lactiplantibacillus plantarum*. *Front. Microbiol.* **12**, 772585. https://doi.org/10.3389/fmicb.2021.772585 (2021).
36. Dubois, M., Gilles, K. A., Hamilton, J. K., Rebers, P. A. & Smith, F. Colorimetric method for determination of sugars and related substances. *Anal. Chem.* **28**, 350–356. https://doi.org/10.1021/ac60111a017 (1956).
37. Dodgson, K. S. & Price, R. G. A note on the determination of the ester sulphate content of sulphated polysaccharides. *Biochem. J.* **84**, 106–110. https://doi.org/10.1042/bj0840106 (1962).
38. Chew, Y. L., Lim, Y. Y., Omar, M. & Khoo, K. S. Antioxidant activity of three edible seaweeds from two areas in South East Asia. *LWT Food Sci. Technol.* **41**, 1067–1072. https://doi.org/10.1016/j.lwt.2007.06.013
39. Zhao, D., Xu, J. & Xu, X. Bioactivity of fucoidan extracted from *Laminaria Japonica* using a novel procedure with high yield. *Food Chem.* **245**, 911–918. https://doi.org/10.1016/j.foodchem.2017.11.083 (2018).
40. Qin, L. et al. Structural characterization of a sulfated polysaccharide from *Ishige Okamurae* and its effect on recovery from immunosuppression. *Int. J. Biol. Macromol.* **236**, 123948. https://doi.org/10.1016/j.ijbiomac.2023.123948 (2023).
41. Fiol, M. et al. Thermal-induced changes of Kale's antioxidant activity analyzed by HPLC-UV/Vis-online-TEAC detection. *Food Chem.* **138**, 857–865. https://doi.org/10.1016/j.foodchem.2012.10.101 (2013).
42. Dudonné, S., Vitrac, X., Coutière, P., Woillez, M. & Mérillon, J. M. Comparative study of antioxidant properties and total phenolic content of 30 plant extracts of industrial interest using DPPH, ABTS, FRAP, SOD, and ORAC assays. *J. Agric. Food Chem.* **57**, 1768–1774. https://doi.org/10.1021/jf803011r (2009).
43. Anastyuk, S. D. et al. ESIMS analysis of fucoidan preparations from *Costaria costata*, extracted from Alga at different life-stages. *Carbohydr. Polym.* **90**, 993–1002. https://doi.org/10.1016/j.carbpol.2012.06.033 (2012).
44. Hu, P. et al. Structural Elucidation and protective role of a polysaccharide from *Sargassum fusiforme* on ameliorating learning and memory deficiencies in mice. *Carbohydr. Polym.* **139**, 150–158. https://doi.org/10.1016/j.carbpol.2015.12.019 (2016).
45. Wei, X. Q. et al. Chain conformation and biological activities of hyperbranched fucoidan derived from brown algae and its desulfated derivative. *Carbohydr. Polym.* **208**, 86–96. https://doi.org/10.1016/j.carbpol.2018.12.060 (2019).
46. Wu, S. Y. et al. Structural characterization and antagonistic effect against P-selectin-mediated function of SFF-32, a fucoidan fraction from *Sargassum fusiforme*. *J. Ethnopharmacol.* **295**, 115408. https://doi.org/10.1016/j.jep.2022.115408 (2022).
47. Yang, Y. J., Hu, T., Li, J. J., Xin, M. & Zhao, X. Structural characterization and effect on leukopenia of fucoidan from *Durvillaea Antarctica*. *Carbohydr. Polym.* **256**, 117529. https://doi.org/10.1016/j.carbpol.2020.117529 (2021).
48. Wang, L. L. et al. Structural characterization of a fucoidan from *Ascophyllum nodosum* and comparison of its protective effect against cellular oxidative stress with its analogues. *Int. J. Biol. Macromol.* **239**, 124295. https://doi.org/10.1016/j.ijbiomac.2023.124295 (2023).
49. Duarte, M. E., Cardoso, M. A., Noseda, M. D. & Cerezo, A. Structural studies on fucoidans from the brown seaweed *Sargassum stenophyllum*. *Carbohydr. Res.* **333**, 281–293. https://doi.org/10.1016/s0008-6215(01)00149-5 (2001).
50. Liu, X. et al. Structural characterization of a P-selectin and EGFR dual-targeting fucoidan from *Sargassum fusiforme*. *Int. J. Biol. Macromol.* **199**, 86–95. https://doi.org/10.1016/j.ijbiomac.2021.12.135 (2022).
51. Fernando, I. P. S. et al. A fucoidan fraction purified from *Chnoospora minima*: A potential inhibitor of LPS-induced inflammatory responses. *Int. J. Biol. Macromol.* **104**, 1185–1193. https://doi.org/10.1016/j.ijbiomac.2017.07.031 (2017).
52. Wang, J., Zhang, Q. B., Zhang, Z. S., Zhang, H. & Niu, X. Z. Structural studies on a novel Fucogalactan sulfate extracted from the brown seaweed *Laminaria Japonica*. *Int. J. Biol. Macromol.* **47**, 126–131. https://doi.org/10.1016/j.ijbiomac.2010.05.010 (2010).
53. Gutierrez, A. L. S. et al. Characterization of glycoinositol phosphoryl ceramide structure mutant strains of *Cryptococcus neoformans*. *Glycobiology* **17**, 1–11. https://doi.org/10.1093/glycob/cwm030 (2007).
54. Li, C. X. et al. Structural, biosynthetic, and serological cross-reactive Elucidation of capsular polysaccharides from *Streptococcus pneumoniae* serogroup 16. *J. Bacteriol.* **201**, 10–1128 (2019). 10.1128/JB.00453 – 19.
55. Haroun-Bouhedja, F., Ellouali, M., Sinquin, C. & Boisson-Vidal, C. Relationship between sulfate groups and biological activities of fucans. *Thromb. Res.* **100**, 453–459. https://doi.org/10.1016/s0049-3848(00)00338-8 (2000).
56. Kasai, A., Arafuka, S., Koshiba, N., Takahashi, D. & Toshima, K. Systematic synthesis of low-molecular weight fucoidan derivatives and their effect on cancer cells. *Org. Biomol. Chem.* **13**, 10556–10568. https://doi.org/10.1039/c5ob01634g (2015).
57. Li, B., Lu, F., Wei, X. J. & Zhao, R. X. Fucoidan structure and bioactivity. *Molecules* **13**, 1671–1695. https://doi.org/10.3390/molecules13081671 (2008).
58. Geun Lee, H. G. et al. Antioxidant potential of low molecular weight fucoidans from *Sargassum autumnale* against H_2O_2-induced oxidative stress in vitro and in zebrafish models based on molecular weight changes. *Food Chem.* **384**, 132591. https://doi.org/10.1016/j.foodchem.2022.132591 (2022).

59. Jia, J. H. et al. Fucoidan from *Scytosiphon lomentaria* protects against destruction of intestinal barrier, inflammation and lipid abnormality by modulating the gut microbiota in dietary fibers-deficient mice. *Int. J. Biol. Macromol.* **224**, 556–567. https://doi.org/10.1016/j.ijbiomac.2022.10.144 (2023).
60. Ajisaka, K., Yokoyama, T. & Matsuo, K. Structural characteristics and antioxidant activities of fucoidans from five brown seaweeds. *J. Appl. Glycosci.* **63**, 31–37. https://doi.org/10.5458/jag.jag.JAG-2015_024 (2016).
61. Ashayerizadeh, O., Dastar, B. & Pourashouri, P. Study of antioxidant and antibacterial activities of depolymerized fucoidans extracted from *Sargassum tenerrimum*. *Int. J. Biol. Macromol.* **151**, 1259–1266. https://doi.org/10.1016/j.ijbiomac.2019.10.172 (2019).
62. El Rashed, Z. E. et al. Antioxidant and antisteatotic activities of a new fucoidan extracted from *Ferula hermonis* roots harvested on Lebanese mountains. *Molecules* **26**, 1161. https://doi.org/10.3390/molecules26041161 (2021).
63. Somasundaram, S. N., Shanmugam, S., Subramanian, B. & Jaganathan, R. Cytotoxic effect of fucoidan extracted from *Sargassum cinereum* on colon cancer cell line HCT-15. *Int. J. Biol. Macromol.* **91**, 1215–1223. https://doi.org/10.1016/j.ijbiomac.2016.06.084 (2016).
64. Jin, W. H. et al. Structural characteristics and anti-complement activities of polysaccharides from *Sargassum Hemiphyllum*. *Glycoconj. J.* **37**, 553–563. https://doi.org/10.1007/s10719-020-09928-w (2020).
65. Wang, J., Zhang, Q. B., Zhang, Z. S. & Li, Z. Antioxidant activity of sulfated polysaccharide fractions extracted from *Laminaria Japonica*. *Int. J. Biol. Macromol.* **42**, 127–132. https://doi.org/10.1016/j.ijbiomac.2007.10.003 (2008).
66. Husni, A. et al. Characteristics and antioxidant activity of fucoidan from sargassum hystrix: Effect of extraction method. *Int. J. Food Sci.* **2022**, 3689724. https://doi.org/10.1155/2022/3689724 (2022).
67. Wu, T. C. et al. Degradation of *Sargassum crassifolium* fucoidan by ascorbic acid and hydrogen peroxide, and compositional, structural, and in vitro anti-lung cancer analyses of the degradation products. *Mar. Drugs.* **18**, 334. https://doi.org/10.3390/md18060334 (2020).
68. Mabate, B., Daub, C. D., Pletschke, B. I. & Edkins, A. L. Comparative analyses of fucoidans from South African brown seaweeds that inhibit adhesion, migration, and long-term survival of colorectal cancer cells. *Mar. Drugs* **21**, 203. https://doi.org/10.3390/md21040203 (2023).
69. Oliveira, C. et al. Fucoidan from *Fucus vesiculosus* inhibits new blood vessel formation and breast tumor growth in vivo. *Carbohydr. Polym.* **223**, 115034. https://doi.org/10.1016/j.carbpol.2019.115034 (2019).
70. Suresh, V. et al. Stabilization of mitochondrial and microsomal function of fucoidan from *Sargassum plagiophyllum* in diethylnitrosamine induced hepatocarcinogenesis. *Carbohydr. Polym.* **92**, 1377–1385. https://doi.org/10.1016/j.carbpol.2012.10.038 (2013).
71. Abdollah, M. R. A., Ali, A. A., Elgohary, H. H. & Elmazar, M. M. Antiangiogenic drugs in combination with seaweed fucoidan: A mechanistic in vitro and in vivo study exploring the VEGF receptor and its downstream signaling molecules in hepatic cancer. *Front. Pharmacol.* **14**, 1108992. https://doi.org/10.3389/fphar.2023.1108992 (2023).
72. Edoo, M. I. A. et al. Serum biomarkers AFP, CEA and CA19-9 combined detection for early diagnosis of hepatocellular carcinoma. *Iran. J. Public. Health* **48**, 314–322 (2019).
73. Wang, T. et al. Targeting neurokinin-3 receptor: A novel anti-angiogenesis strategy for cancer treatment. *Oncotarget* **8**, 40713–40723. https://doi.org/10.18632/oncotarget.17250 (2017).
74. Li, D. et al. Dual blockade of vascular endothelial growth factor (VEGF) and basic fibroblast growth factor (FGF-2) exhibits potent anti-angiogenic effects. *Cancer Lett.* **377**, 164–173. https://doi.org/10.1016/j.canlet.2016.04.036 (2016).
75. Zhu, C. et al. Fucoidan inhibits the growth of hepatocellular carcinoma independent of angiogenesis. *Evid. Based Complement. Alternat. Med. eCAM* **2013**, 692549 (2013). https://doi.org/10.1155/2013/692549 (2013).
76. Bertacchini, J. et al. Targeting PI3K/AKT/mTOR network for treatment of leukemia. *Cell. Mol. Life Sci.* **72**, 2337–2347. https://doi.org/10.1007/s00018-015-1867-5 (2015).
77. Lien, E. C., Dibble, C. C. & Toker, A. PI3K signaling in cancer: Beyond AKT. *Curr. Opin. Cell. Biol.* **45**, 62–71. https://doi.org/10.1016/j.ceb.2017.02.007 (2017).
78. Lee, H., Kim, J. S. & Kim, E. Fucoidan from seaweed *Fucus vesiculosus* inhibits migration and invasion of human lung cancer cell via PI3K-Akt-mTOR pathways. *PLOS ONE* **7**, e50624. https://doi.org/10.1371/journal.pone.0050624 (2012).
79. Chi, J. et al. Studies on anti-hepatocarcinoma effect, pharmacokinetics and tissue distribution of carboxymethyl Chitosan based Norcantharidin conjugates. *Carbohydr. Polym.* **226**, 115297. https://doi.org/10.1016/j.carbpol.2019.115297 (2019).
80. Haruki, K. et al. Inhibition of nuclear factor-κB enhances the antitumor effect of tumor necrosis factor-α gene therapy for hepatocellular carcinoma in mice. *Surgery* **154**, 468–478. https://doi.org/10.1016/j.surg.2013.05.037 (2013).
81. Larmonier, N. et al. The Inhibition of TNF-alpha anti-tumoral properties by blocking antibodies promotes tumor growth in a rat model. *Exp. Cell. Res.* **313**, 2345–2355. https://doi.org/10.1016/j.yexcr.2007.03.027 (2007).
82. Lanaya, H. et al. EGFR has a tumour-promoting role in liver macrophages during hepatocellular carcinoma formation. *Nat. Cell. Biol.* **16**, 972–977. https://doi.org/10.1038/ncb3031 (2014).

Author contributions

Q.Y.: Investigation, formal analysis, data curation and writing-original draft. Y.L.: Investigation, formal analysis and data curation. F.L.: Investigation and formal analysis. T.H.: Investigation and formal analysis. S.G.: Investigation and formal analysis. M.C.:Investigation and formal analysis. L.Z.: Formal analysis and methodology. L.S.: Methodology. S.Z.: Data curation. C.Z.: Formal analysis and methodology. K.L.: Conceptualization, Project administration and funding acquisition.

Funding

This work was supported by the Key Technology Research and Development Program of Shandong Province (Competitive provincial innovation platform project) [grant number 2023CXPT037]; Innovation capability improvement project for SMEs of Shandong Province [grant number 2022TSGC1076]; and the XPCC Financial Science and Technology Project in 2022 [grant number 2022AB002].

Declarations

Competing interests

The authors declare no competing interests.

Additional information

Supplementary Information The online version contains supplementary material available at https://doi.org/10.1038/s41598-025-94312-7.

Correspondence and requests for materials should be addressed to Q.Y. or K.L.